Lamya H. Al-Wahaibi, Hazem A. Ghabbour, Fatmah A. M. Al-Omary, Edward R. T. Tiekink and Ali A. El-Emam*

Crystal structure of 5-(adamantan-1-yl)-3-[(4-trifluoromethylanilino)methyl]-2,3-dihydro-1,3,4-oxadiazole-2-thione, $C_{20}H_{22}F_3N_3OS$

https://doi.org/10.1515/ncrs-2022-0144
Received March 26, 2022; accepted April 21, 2022;
published online May 5, 2022

Abstract

$C_{20}H_{22}F_3N_3OS$, triclinic, $P\bar{1}$ (no. 1), a = 6.9678(8) Å, b = 10.7614(14) Å, c = 13.0503(14) Å, α = 76.870(3)°, β = 88.004(4)°, γ = 87.275(4)°, V = 951.60(19) Å^3, Z = 2, $R_{gt}(F)$ = 0.0629, $wR_{ref}(F^2)$ = 0.1626, T = 100 K.

CCDC no.: 1425854

Table 1 contains crystallographic data and Table 2 contains the list of the atoms including atomic coordinates and displacement parameters.

Source of material

Formaldehyde solution (37%, 1.5 mL) and 4-trifluoromethylaniline (1.61 g, 0.01 mol) were added to a solution of 5-(adamantan-1-yl)-1,3,4-oxadiazole-2(3*H*)-thione (2.36 g, 0.01 mol) in ethanol (15 mL), and the mixture was stirred at 293 K for 2 h and allowed to stand overnight. The precipitated crude product was filtered, washed with water, dried and crystallised from aqueous ethanol to yield 3.36 g (82%) of the title compound as colourless prisms. M.pt: 447–449 K (uncorrected). **Anal. Calc**. for $C_{20}H_{22}F_3N_3OS$: C, 58.67; H, 5.42; N, 10.26; S, 7.83%. Found: C, 58.63; H, 5.45;

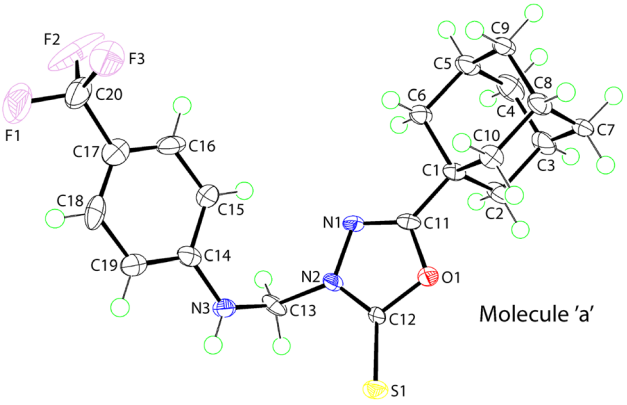

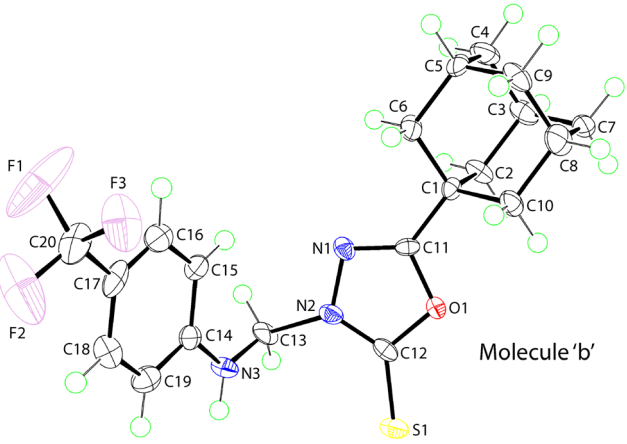

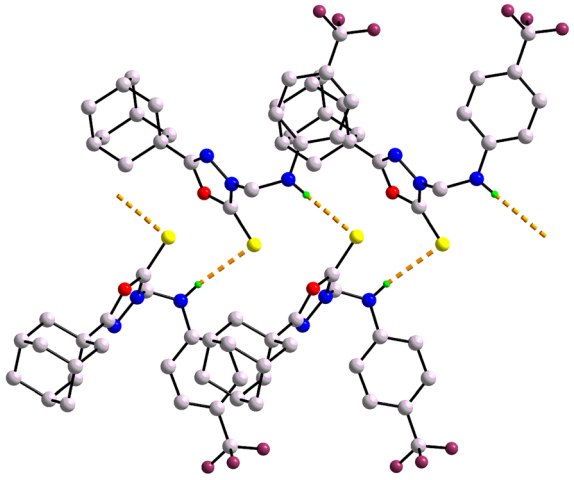

***Corresponding author: Ali A. El-Emam**, Department of Medicinal Chemistry, Faculty of Pharmacy, Mansoura University, Mansoura 35516, Egypt, E-mail: elemam5@hotmail.com. https://orcid.org/0000-0002-9325-9497
Lamya H. Al-Wahaibi, Department of Chemistry, College of Sciences, Princess Nourah bint Abdulrahman University, Riyadh 11671, Saudi Arabia
Hazem A. Ghabbour, Department of Medicinal Chemistry, Faculty of Pharmacy, Mansoura University, Mansoura 35516, Egypt
Fatmah A. M. Al-Omary, Department of Pharmaceutical Chemistry, College of Pharmacy, King Saud University, Riyadh 11451, Saudi Arabia
Edward R. T. Tiekink, Research Centre for Crystalline Materials, School of Medical and Life Sciences, Sunway University, No. 5 Jalan Universiti, 47500 Bandar Sunway, Selangor Darul Ehsan, Malaysia

Table 1: Data collection and handling.

Crystal:	Colourless prism
Size:	0.54 × 0.23 × 0.11 mm
Wavelength:	Mo *K*α radiation (0.71073 Å)
μ:	0.22 mm^{-1}
Diffractometer, scan mode:	Bruker APEX-II D8 venture, φ and ω
θ_{max}, completeness:	25.0°, >99%
$N(hkl)_{measured}$, $N(hkl)_{unique}$, R_{int}:	21,069, 6660, 0.041
Criterion for I_{obs}, $N(hkl)_{gt}$:	$I_{obs} > 2\sigma(I_{obs})$, 6248
$N(param)_{refined}$:	511
Programs:	Bruker [1], SHELX [2, 3], WinGX/ORTEP [4]

Table 2: Fractional atomic coordinates and isotropic or equivalent isotropic displacement parameters (Å^2).

Atom	*x*	*y*	*z*	U_{iso}*/U_{eq}
S1A	0.3734 (2)	−0.06030 (14)	0.44740 (12)	0.0166 (4)
O1A	0.1263 (6)	0.0610 (4)	0.3004 (3)	0.0131 (9)
N1A	0.0897 (7)	0.2555 (5)	0.3300 (4)	0.0136 (11)
N2A	0.2170 (7)	0.1807 (5)	0.4005 (4)	0.0133 (10)
N3A	0.4741 (7)	0.2654 (5)	0.4833 (4)	0.0153 (11)
H3AB	0.572 (7)	0.215 (6)	0.510 (5)	0.018*
F1A	0.8885 (10)	0.7712 (6)	0.2557 (4)	0.0644 (19)
F2A	0.5965 (10)	0.8309 (5)	0.2232 (5)	0.0644 (18)
F3A	0.7488 (7)	0.7206 (4)	0.1308 (3)	0.0379 (11)
C1A	−0.1006 (9)	0.2087 (6)	0.1860 (4)	0.0131 (13)
C2A	−0.2851 (9)	0.1361 (7)	0.2270 (5)	0.0188 (14)
H2AA	−0.254193	0.043201	0.247696	0.023*
H2AB	−0.338981	0.164466	0.289477	0.023*
C3A	−0.4324 (9)	0.1639 (7)	0.1390 (5)	0.0211 (14)
H3AA	−0.551853	0.117547	0.164934	0.025*
C4A	−0.4816 (9)	0.3078 (7)	0.1086 (5)	0.0235 (15)
H4AA	−0.578978	0.325877	0.053066	0.028*
H4AB	−0.535929	0.337093	0.170541	0.028*
C5A	−0.2999 (10)	0.3787 (6)	0.0684 (5)	0.0193 (14)
H5AA	−0.332776	0.472425	0.048326	0.023*
C6A	−0.1501 (9)	0.3533 (6)	0.1556 (5)	0.0157 (13)
H6AA	−0.202663	0.382915	0.217727	0.019*
H6AB	−0.032805	0.400366	0.129951	0.019*
C7A	−0.3492 (10)	0.1177 (6)	0.0425 (5)	0.0182 (14)
H7AA	−0.316444	0.024952	0.062525	0.022*
H7AB	−0.445849	0.132579	−0.013265	0.022*
C8A	−0.1686 (10)	0.1909 (6)	0.0014 (5)	0.0179 (13)
H8AA	−0.114654	0.161871	−0.061632	0.022*
C9A	−0.2162 (9)	0.3350 (6)	−0.0287 (5)	0.0170 (13)
H9AA	−0.310615	0.354184	−0.085687	0.020*
H9AB	−0.098380	0.381364	−0.054519	0.020*
C10A	−0.0181 (9)	0.1631 (6)	0.0893 (5)	0.0153 (13)
H10A	0.014370	0.070330	0.109004	0.018*
H10B	0.100871	0.208062	0.063410	0.018*
C11A	0.0406 (8)	0.1820 (6)	0.2727 (4)	0.0116 (12)
C12A	0.2407 (8)	0.0624 (6)	0.3843 (4)	0.0103 (12)
C13A	0.2859 (9)	0.2254 (6)	0.4916 (5)	0.0158 (13)
H13A	0.199478	0.297127	0.502702	0.019*
H13B	0.274240	0.155203	0.555075	0.019*
C14A	0.5328 (9)	0.3822 (6)	0.4224 (5)	0.0143 (13)
C15A	0.4044 (10)	0.4654 (6)	0.3557 (5)	0.0194 (14)
H15A	0.275917	0.442040	0.350387	0.023*
C16A	0.4670 (11)	0.5816 (6)	0.2979 (5)	0.0220 (15)
H16A	0.379578	0.639995	0.255293	0.026*
C17A	0.6570 (11)	0.6128 (7)	0.3021 (5)	0.0223 (15)
C18A	0.7850 (10)	0.5317 (7)	0.3681 (5)	0.0216 (15)
H18A	0.914460	0.553968	0.371951	0.026*
C19A	0.7184 (9)	0.4165 (6)	0.4287 (5)	0.0172 (13)
H19A	0.803501	0.360982	0.475187	0.021*
C20A	0.7246 (12)	0.7329 (7)	0.2305 (6)	0.0302 (18)
S1B	0.8594 (2)	1.06071 (14)	0.55707 (12)	0.0181 (4)
O1B	0.6111 (6)	0.9361 (4)	0.7018 (3)	0.0121 (9)
N1B	0.6062 (7)	0.7430 (5)	0.6693 (4)	0.0138 (11)
N2B	0.7321 (7)	0.8202 (5)	0.6002 (4)	0.0144 (11)
N3B	1.0073 (8)	0.7352 (5)	0.5130 (4)	0.0166 (11)
H3BB	1.098 (8)	0.787 (6)	0.484 (5)	0.020*
F1B	1.1988 (13)	0.1684 (5)	0.7620 (5)	0.081 (2)
F2B	1.4793 (10)	0.2431 (6)	0.7529 (4)	0.072 (2)
F3B	1.2775 (7)	0.2737 (5)	0.8712 (3)	0.0413 (12)
C1B	0.3907 (9)	0.7883 (6)	0.8138 (5)	0.0116 (12)
C2B	0.1965 (9)	0.8522 (7)	0.7710 (5)	0.0171 (13)
H2BA	0.209521	0.945584	0.746741	0.021*
H2BB	0.159649	0.818357	0.710316	0.021*
C3B	0.0406 (9)	0.8245 (7)	0.8585 (5)	0.0197 (14)
H3BA	−0.084207	0.866512	0.831068	0.024*
C4B	0.0191 (9)	0.6804 (7)	0.8921 (5)	0.0227 (15)
H4BA	−0.084525	0.661078	0.946554	0.027*
H4BB	−0.016148	0.646910	0.830956	0.027*
C5B	0.2072 (10)	0.6167 (6)	0.9358 (5)	0.0182 (14)
H5BA	0.191746	0.522441	0.958370	0.022*
C6B	0.3673 (10)	0.6434 (6)	0.8500 (5)	0.0187 (14)
H6BA	0.489875	0.601295	0.878336	0.022*
H6BB	0.333932	0.608230	0.789419	0.022*
C7B	0.0991 (10)	0.8778 (6)	0.9527 (5)	0.0199 (14)
H7BA	0.114163	0.971073	0.929898	0.024*
H7BB	−0.002375	0.862112	1.008562	0.024*
C8B	0.2873 (10)	0.8127 (7)	0.9953 (5)	0.0242 (15)
H8BA	0.323632	0.846582	1.056910	0.029*
C9B	0.2664 (10)	0.6671 (6)	1.0307 (5)	0.0198 (14)
H9BA	0.389877	0.625215	1.057680	0.024*
H9BB	0.167595	0.647761	1.087787	0.024*
C10B	0.4459 (9)	0.8404 (6)	0.9099 (5)	0.0168 (13)
H10C	0.569004	0.799209	0.938070	0.020*
H10D	0.462561	0.933660	0.887926	0.020*
C11B	0.5385 (8)	0.8157 (6)	0.7282 (4)	0.0116 (12)
C12B	0.7359 (8)	0.9358 (6)	0.6192 (5)	0.0136 (13)
C13B	0.8156 (9)	0.7771 (6)	0.5067 (5)	0.0168 (13)
H13C	0.738634	0.706928	0.494871	0.020*
H13D	0.801939	0.848788	0.444338	0.020*
C14B	1.0726 (9)	0.6173 (6)	0.5754 (5)	0.0157 (13)
C15B	0.9477 (10)	0.5316 (6)	0.6376 (5)	0.0183 (13)
H15B	0.813251	0.550759	0.638783	0.022*
C16B	1.0248 (10)	0.4166 (7)	0.6984 (5)	0.0216 (15)
H16B	0.940911	0.356650	0.739494	0.026*
C17B	1.2184 (11)	0.3892 (6)	0.6996 (5)	0.0214 (15)

Table 2: (continued)

Atom	x	y	z	U_{iso}*/U_{eq}
C18B	1.3421 (9)	0.4726 (6)	0.6362 (5)	0.0183 (14)
H18B	1.476321	0.452406	0.635334	0.022*
C19B	1.2684 (10)	0.5859 (6)	0.5737 (5)	0.0188 (14)
H19B	1.352845	0.642595	0.529361	0.023*
C20B	1.2923 (12)	0.2697 (7)	0.7700 (5)	0.0284 (17)

N, 10.24; S, 7.82%. **^{1}H-NMR** ($CDCl_3$, 500.13 MHz): δ 1.74–1.80 (m, 6H, Adamantane-H), 1.97–1.99 (m, 6H, Adamantane-H), 2.12 (s, 3H, Adamantane-H), 5.46 (s, 1H, NH), 5.78 (d, 2H, CH_2, J = 6.8 Hz), 6.96 (d, 2H, Ar–H, J = 8.5 Hz), 7.43 (d, 2H, Ar–H, J = 8.5 Hz). **^{13}C-NMR** ($CDCl_3$, 125.76 MHz): δ 27.41, 34.33, 36.04, 39.04 (adamantane–C), 59.0 (CH_2), 123.85 (CF_3), 114.50, 119.88, 128.09, 147.12 (Ar–C), 165.45 (oxadiazole–C), 177.43 (C=S). **ESI-MS** m/z: 410.3 $[M + H]^+$.

Experimental details

The C-bound H atoms were geometrically placed (C–H = 0.95–1.00 Å) and refined as riding with U_{iso}(H) = 1.2U_{eq}(C). The N-bound H atoms were located from a difference Fourier map and refined with N–H = 0.88 + –0.01 Å, and with U_{iso}(H) set to 1.2U_{eq}(N).

Comment

The highly lipophilic adamantane cage is frequently found in biologically-active compounds possessing various pharmacological activities [5–7]. Amantadine was discovered early as an efficient drug for the control of Influenza A infection [8, 9] and further approved for the treatment of Parkinson's disease [10]. Further studies based on adamantane derivatives resulted in the evolution of more active anti-viral drugs such as tromantadine [11] and rimantadine [12]. Adamantane-based analogues were also reported to display significant inhibitory effects against human immunodeficiency virus (HIV) [13–15]. The adamantane ethylenediamine analogue, SQ109, and the related dipiperidine derivative, SQ609, were further approved as efficient therapies against drug-susceptible and drug-resistant *Mycobacterium tuberculosis* strains [16, 17]. The adamantane carboxamide derivative Opaganib (ABC294640) is a newly approved anti-tumour drug for treating patients suffering from advanced solid tumours [18–20]. Furthermore, various adamantane derivatives were recognised as efficient antibacterial and anti-fungal candidates [21–24]. On the other hand, the 1,3,4-oxadiazole nucleus was reported to constitute the core of several chemotherapeutic agents possessing anti-bacterial [25, 26], anti-fungal [27], anti-cancer [28, 29] and anti-viral [30] activities. Besides, 1,3,4-oxadiazole derivatives are presently utilised as safe herbicides for crop protection [31]. In an earlier study, we described the synthesis, anti-HIV, and anti-bacterial activities of adamantane-1,3,4-oxadiazole hybrid N-Mannich bases [15]. The previously reported compounds showed strong inhibitory activity against Gram-positive bacteria and limited activity against Gram-negative bacteria. The anti-bacterial structure-activity relationship of these compounds proved that the spectrum of the anti-bacterial efficacy is fundamentally contingent on the nature of the substituents of the aryl moiety. Further optimisation studies based on the previously prepared compounds resulted in development of the title compound (I), which exhibited strong broad-spectrum anti-bacterial activity.

The molecular structures of the independent molecules, i.e. molecule a and molecule b, comprising the crystallographic asymmetric-unit of (I) are shown in the figure (70% probability ellipsoids). The independent molecules resemble each other very closely as seen in the r.m.s. bond and angle fits of 0.0128 Å and 0.745°, respectively [32]. Crucially, there is no pseudo centre of inversion between the molecules, they being directly superimposable.

Each molecule comprises a central, planar 1,3,4-oxadiazole core connected to a thione–S [1.649(6) & 1.665(6) Å for molecules a and b, respectively], an N-bound (4-trifluoromethylanilino)methyl group and the remaining carbon atom carries the adamantan-1-yl group. Within the five-membered ring, the C11–N1 bond of 1.270(8) Å is significantly shorter than the C12–N2 bond of 1.339(8) Å, and the C11–O1 [1.383(7) Å] and C12–O1 [1.379(7) Å] bond lengths are experimentally equivalent, results suggesting limited delocalisation of π-electron density in the ring; the equivalent bond lengths for molecule b are 1.280(8), 1.324(8), 1.379(7) and 1.361(7) Å, respectively. The dihedral angle between the five- and six-membered rings is 47.1(3)°; the equivalent angle for molecule b is 51.3(3)°. Globally, the two central ring-substituents tend to be oriented to the same side of the molecule in a direction away from the thione-S atom.

There are four closely related structures in the literature, namely the phenyl compound, i.e. the parent compound [33], the 4-fluorophenyl [34], the 4-chlorophenyl [35] and the 2-trifluoromethyl [36] derivatives. Each of the previously reported structure resemble that noted above for (I).

The most prominent feature of the molecular packing in the crystal of (I) is a twisted chain aligned along the *a*-axis. The chains comprise alternating independent molecules

and feature amine-N–H···S(thione) hydrogen bonds [N3a–H3ab···S1b^{i}: H3ab···S1b^{i} = 2.54(6) Å, N3a–H3ab···S1b^{i} = 3.412(5) Å with angle at H3ab = 171(6)° and N3b–H3bb···S1a^{ii}: H3bb···S1a^{ii} = 2.55(6) Å, N3b–H3bb···S1a^{ii} = 3.407(6) Å with angle at H3bb = 166(5)° for symmetry operations (i): x, $-1+y$, z and (ii): $1+x$, $1+y$, z]. A portion of the supramolecular chain is shown in the lower view of the Figure, where the hydrogen bonds are shown as dashed lines and non-participating hydrogen atoms are omitted.

As indicated above, the molecular structures are very similar as is the primary mode of association between the molecules. This is confirmed by the calculation of the Hirshfeld surfaces and the full and decomposed two-dimensional fingerprint plots. Crystal Explorer 17 [37] was employed for this purpose following established procedures [38]. The differences between the Hirshfeld surfaces for each independent molecule differ by no more than 1%. The most significant contribution are from H···H contacts being 39.9 and 39.2% for molecules a and b, respectively. The next most important contributions are of the type F···H/H···F, i.e. 24.5 and 24.0%, respectively. There are also significant contributions to the Hirshfeld surface by C···H/H···C [13.6 and 13.9%], S···H/H···S [9.0 and 9.8%], N···H/H···N [4.1 and 4.3%] and O···H/H···O [3.4 and 3.5%]. The only other surface contacts greater than 1.0% are S···F/F···S [1.5 and 0.9%], S···N/N···S [1.2 and 1.2%] and S···C/C···S [1.0 and 1.0%].

Acknowledgements: This research was funded by the Princess Nourah bint Abdulrahman University Researchers Supporting Project No. PNURSP2022R3, Princess Nourah bint Abdulrahman University, Riyadh, Saudi Arabia.

Author contributions: All the authors have accepted responsibility for the entire content of this submitted manuscript and approved submission.

Research funding: Princess Nourah bint Abdulrahman University Researchers Supporting Project No. PNURSP2022R3, Princess Nourah bint Abdulrahman University, Riyadh, Saudi Arabia.

Conflict of interest statement: The authors declare no conflicts of interest regarding this article.

References

1. Bruker. SADABS, APEX2 and SAINT; Bruker AXS Inc.: Madison, Wisconsin, USA, 2014.
2. Sheldrick G. M. A short history of *SHELX*. *Acta Crystallogr.* 2008, *A64*, 112–122.
3. Sheldrick G. M. Crystal structure refinement with SHELXL. *Acta Crystallogr.* 2015, *C71*, 3–8.
4. Farrugia L. J. WinGX and ORTEP for Windows: an update. *J. Appl. Crystallogr.* 2012, *45*, 849–854.
5. Wanka L., Iqbal K., Schreiner P. R. The lipophilic bullet hits the targets: medicinal chemistry of adamantane derivatives. *Chem. Rev.* 2013, *113*, 3516–3604.
6. Liu J., Obando D., Liao V., Lifa T., Codd R. The many faces of the adamantyl group in drug design. *Eur. J. Med. Chem.* 2011, *46*, 1949–1963.
7. Lamoureux G., Artavia G. Use of the adamantane structure in medicinal chemistry. *Curr. Med. Chem.* 2010, *17*, 2967–2978.
8. Davies W. L., Grunert R. R., Haff R. F., McGahen J. W., Neumayer E. M., Paulshock M., Watts J. C., Wood T. R., Hermann E. C., Hoffmann C. E. Antiviral activity of 1-adamantamine (amantadine). *Science* 1964, *144*, 862–863.
9. Wendel H. A., Snyder M. T., Pell S. Trial of amantadine in epidemic influenza. *Clin. Pharmacol. Ther.* 1966, *7*, 38–43.
10. Schwab R. S., England A. C. Jr., Poskanzer D. C., Young R. R. Amantadine in the treatment of Parkinson's disease. *J. Am. Med. Assoc.* 1969, *208*, 1168–1170.
11. Rosenthal K. S., Sokol M. S., Ingram R. L., Subramanian R., Fort R. C. Tromantadine: Inhibitor of early and late events in herpes simplex virus replication. *Antimicrob. Agents Chemother.* 1982, *22*, 1031–1036.
12. Wingfield W. L., Pollack D., Grunert R. R. Therapeutic efficacy of amantadine HCl and rimantadine HCl in naturally occurring influenza A2 respiratory Illness in man. *N. Engl. J. Med.* 1969, *281*, 579–584.
13. Balzarini J., Orzeszko-Krzesińska B., Maurin J. K., Orzeszko A. Synthesis and anti-HIV studies of 2- and 3-adamantyl-substituted thiazolidin-4-ones. *Eur. J. Med. Chem.* 2009, *44*, 303–311.
14. Balzarini J., Orzeszko B., Mauri J. K., Orzeszko A. Synthesis and anti-HIV studies of 2-adamantyl-substituted thiazolidin-4-ones. *Eur. J. Med. Chem.* 2007, *42*, 993–1003.
15. El-Emam A. A., Al-Deeb O. A., Al-Omar M., Lehmann J. Synthesis, antimicrobial, and anti-HIV-1 activity of certain 5-(1-adamantyl)-2-substituted thio-1,3,4-oxadiazoles and 5-(1-adamantyl)-3-substituted aminomethyl-1,3,4-oxadiazoline-2-thiones. *Bioorg. Med. Chem.* 2004, *12*, 5107–5113.
16. Protopopova M., Hanrahan C., Nikonenko B., Samala R., Chen P., Gearhart J., Einck L., Nacy C. A. Identification of a new antitubercular drug candidate, SQ109, from a combinatorial library of 1,2-ethylenediamines. *J. Antimicrob. Chemother.* 2005, *56*, 968–974.
17. Bogatcheva E., Hanrahan C., Nikonenko B., de los Santos G., Reddy V., Chen P., Barbosa F., Einck L., Nacy C., Protopopova M. Identification of SQ609 as a lead compound from a library of dipiperidines. *Bioorg. Med. Chem. Lett.* 2011, *21*, 5353–5357.
18. McNaughton M., Pitman M., Pitson S. M., Pyne N. J., Pyne S. Proteasomal degradation of sphingosine kinase 1 and inhibition of dihydroceramide desaturase by the sphingosine kinase inhibitors, SKi or ABC294640, induces growth arrest in androgen-independent LNCaP-AI prostate cancer cells. *Oncotarget* 2016, *7*, 16663–16675.
19. Britten C. D., Garrett-Mayer E., Chin S. H., Shirai K., Ogretmen B., Bentz T. A., Brisendine A., Anderton K., Cusack S. L., Maines L. W., Zhuang Y., Smith C. D., Thomas M. B. A phase I study of ABC294640, a first-in-class sphingosine kinase-2 inhibitor, in patients with advanced solid tumors. *Clin. Cancer Res.* 2017, *23*, 4642–4650.

20. Zhou J., Chen J., Yu H. Targeting sphingosine kinase 2 by ABC294640 inhibits human skin squamous cell carcinoma cell growth. *Biochem. Biophys. Res. Commun*. 2018, *497*, 535–542.
21. Omar K., Geronikaki A., Zoumpoulakis P., Camoutsis C., Soković M., Ćirić A., Glamočlija J. Novel 4-thiazolidinone derivatives as potential antifungal and antibacterial drugs. *Bioorg. Med. Chem.* 2010, *18*, 426–432.
22. Al-Wahaibi L. H., Hassan H. M., Abo-Kamar A. M., Ghabbour H. A., El-Emam A. A. Adamantane-isothiourea hybrid derivatives: synthesis, characterization, in vitro antimicrobial, and in vivo hypoglycemic activities. *Molecules* 2017, *22*, 710.
23. El-Emam A. A., Al-Tamimi A.-M. S., Al-Omar M. A., Alrashood K. A., Habib E. E. Synthesis and antimicrobial activity of novel 5-(1-adamantyl)-2-aminomethyl-4-substituted-1,2,4-triazoline-3-thiones. *Eur. J. Med. Chem.* 2013, *68*, 96–102.
24. Al-Abdullah E. S., Al-Tuwaijri H. M., Hassan H. M., Haiba M. E. Antimicrobial and hypoglycemic activities of novel N-Mannich bases derived from 5-(1-adamantyl)-4-substituted-1,2,4-triazoline-3-thiones. *Int. J. Mol. Sci.* 2014, *15*, 22995–23010.
25. Ogata M., Atobe H., Kushida H., Yamamoto K. In vitro sensitivity of mycoplasmas isolated from various animals and sewage to antibiotics and nitrofurans. *J. Antibiot.* 1971, *24*, 443–451.
26. Kadi A. A., El-Brollosy N. R., Al-Deeb O. A., Habib E. E., Ibrahim T. M., El-Emam A. A. Synthesis, antimicrobial, and anti-inflammatory activities of novel 2-(1-adamantyl)-5-substituted-1,3,4-oxadiazoles and 2-(1-adamantylamino)-5-substituted-1,3,4-thiadiazoles. *Eur. J. Med. Chem.* 2007, *42*, 235–242.
27. Prakash O., Kumar M., Kumar R., Sharma C., Aneja K. R. Hypervalent iodine(III) mediated synthesis of novel unsymmetrical 2,5-disubstituted 1,3,4-oxadiazoles as antibacterial and antifungal agents. *Eur. J. Med. Chem.* 2010, *45*, 4252–4257.
28. Gamal El-Din M. M., El-Gamal M. I., Abdel-Maksoud M. S., Yoo K. H., Oh C.-H. Synthesis and in vitro antiproliferative activity of new 1,3,4-oxadiazole derivatives possessing sulfonamide moiety. *Eur. J. Med. Chem*. 2015, *90*, 45–52.
29. Zhang K., Wang P., Xuan L.-N., Fu X.-Y., Jing F., Li S., Liu Y.-M., Chen B.-Q. Synthesis and antitumor activities of novel hybrid molecules containing 1,3,4-oxadiazole and 1,3,4-thiadiazole bearing Schiff base moiety. *Bioorg. Med. Chem. Lett* 2014, *24*, 5154–5146.
30. Summa V., Petrocchi A., Bonelli F., Crescenzi B., Donghi M., Ferrara M., Fiore F., Gardelli C., Gonzalez Paz O., Hazuda D. J., Jones P., Kinzel O., Laufer R., Monteagudo E., Muraglia E., Nizi E., Orvieto F., Pace P., Pescatore G., Scarpelli R., Stillmock K., Witmer M. V., Rowley M. Discovery of raltegravir, a potent, selective orally bioavailable HIV-integrase inhibitor for the treatment of HIV-AIDS infection. *J. Med. Chem.* 2008, *51*, 5843–5855.
31. Shi W., Qian X., Zhang R., Song G. Synthesis and quantitative structure-activity relationships of new 2,5-disubstituted-1,3,4-oxadiazoles. *J. Agric. Food Chem.* 2001, *49*, 124–130.
32. Spek A. L. *checkCIF* validation ALERTS: what they mean and how to respond. *Acta Crystallogr.* 2020, *E76*, 1–11.
33. Al-Tamimi A.-M. S., Al-Deeb O. A., El-Emam A. A., Ng S. W., Tiekink E. R. T. 5-(Adamantan-1-yl)-3-anilinomethyl-2,3-dihydro-1,3,4-oxadiazole-2-thione. *Acta Crystallogr.* 2013, *E69*, o729.
34. Al-Tamimi A.-M. S., Alafeefy A. M., El-Emam A. A., Ng S. W., Tiekink E. R. T. 5-(Adamantan-1-yl)-3-[(4-fluoroanilino)methyl]-2,3-dihydro-1,3,4-oxadiazole-2-thione. *Acta Crystallogr.* 2013, *E69*, o730.
35. Al-Alshaikh M. A., Ghabbour H. A., Al-Tamimi A.-M. S., Abdelbaky M. S. M., Garcia-Granda S., El-Emam A. A. Crystal structure of 5-(adamantan-1-yl)-3-[(4-chloroanilino)methyl]-2,3-dihydro-1,3,4-oxadiazole-2-thione, $C_{19}H_{22}ClN_3OS$. *Z. Kristallogr. N. Cryst. Struct.* 2016, *231*, 301–303;.
36. Al-Wabli R. I., El-Emam N. A., Ghabbour H. A., Haress N. G., El-Emam A. A. Crystal structure of 5-(adamantan-1-yl)-3-[(2-trifluoromethylanilino)methyl]-2,3-dihydro-1,3,4-oxadiazole-2-thione, $C_{20}H_{22}F_3N_3OS$. *Z. Kristallogr. N. Cryst. Struct.* 2016, *231*, 815–817.
37. Turner M. J., Mckinnon J. J., Wolff S. K., Grimwood D. J., Spackman P. R., Jayatilaka D., Spackman M. A. *Crystal Explorer v17*; The University of Western Australia: Australia, 2017.
38. Tan S. L., Jotani M. M., Tiekink E. R. T. Utilizing Hirshfeld surface calculations, non-covalent interaction (NCI) plots and the calculation of interaction energies in the analysis of molecular packing. *Acta Crystallogr.* 2019, *E75*, 308–318.